International Journal of Engineering & Technology, 7 (3.29) (2018) 620-626

International Journal of Engineering & Technology

Website: www.sciencepubco.com/index.php/IJET

Research paper

A novel implementation of medical image registration and fusion using ASM-SSIF

Suneetha Rikhari [1] *, Sandeep Jaiswal [1]

[1] ECE Department, College of Engineering & Technology, Mody University of Science and Technology, Rajasthan, India
**Corresponding author E-mail: suneetha.rikhari@gmail.com*

Abstract

In medical imaging a single image of a targeted organ is captured using different imaging modalities such as MR (Magnetic Resonance) and CT (Computed Tomography), to get desired information from the region of interest. For better diagnosis the information obtained from these two modalities has to be combined into a single image. Image fusion is a process of integrating useful or complementary information from multiple images into a single image. In this work, we proposed a novel method for image fusion with biomedical images i.e., MR and CT images, by formulating a convex optimization problem. The optimization problem uses an Active Slope Meagerness (ASM) regularizer with statistics based steered image filtration (SSIF). Precise registration is needed by the MR and CT image fusion, while the misalignment is quite hard to obviate during the preprocessing step. To surmount this, we had proposed a robust and new approach for both registration as well as the fusion of MR and CT images. Our approach focuses on simultaneous registration during the fusion procedure. Initially, the MR image is focalized to enhanced resolution, which permits us for more precise registration of images. At the same time, fusion of images can be done precisely by extinguishing the misalignment gradually. We iteratively persist these two procedures until the convergence. The performance of the algorithm is judged both qualitatively and quantitatively. The Proposed ASM-SSIF method is compared with the existing methods. The simulation results showed that our algorithm has given greater performance by enhancing the overall fusion quality of MR and CT images in terms of image quality assessment. Specifically, our proposed approach is shown to be much more powerful on the medical data sets of real-world with pre-registration errors.

Keywords: *Active Slope Meagerness Regularize; Fast Iterative Shrinkage Thresholding Algorithm; Image Registration; Image Fusion; Image Quality Assessment Metrics; MR and CT Imaging; Steerable Image Filtration; Statistics and Vectorial Total Variation.*

1. Introduction

In medical imaging, different modalities such as Positron Emission Tomography (PET), Single Photon Emission Computed Tomography (SPECT), CT, and MR are used to capture necessary information [1]. Registration plays a vital role in the field of processing of medical images and in the process of surgery which is based on image-guidance due the fact that in these processes, vital and useful data are pulled out from the multiple source images. Hence, the registration process gained more attention from the users due to the acquisition of source images from different sensors in different directions with different time frames [2-6]. The major motivation behind the vitality and usage of registration of medical images is the implementation and usability of promoted surgical techniques in the field of image-guided surgery and radiotherapy. Registration is very much utilized in the applications of remote sensing, and satellite. In addition, it plays a vital in processing of medical images. Integrating useful data from several imaging like MR, CT, PET and SPECT [7] is the main motive of registration in medical image analysis. These modalities were utilized for the analysis of brain images in the beginning stage of implementation. However, now a day it has been spread to all the images those describes human anatomy like the images of heart, breast/chest, knee's surgical treatment, dental implants, retina, thorax, pelvis and abdomen. For example, the data sets shown in Figure 1, consists of CT images (shown on left side) and MR image (shown on right side). The CT image withdraws hard tissue information such as bone and the MR image withdraws soft tissue information. For better diagnosis of the patient the doctor needs both the soft and hard tissue information. Hence there is a need to fuse both MR and CT images.

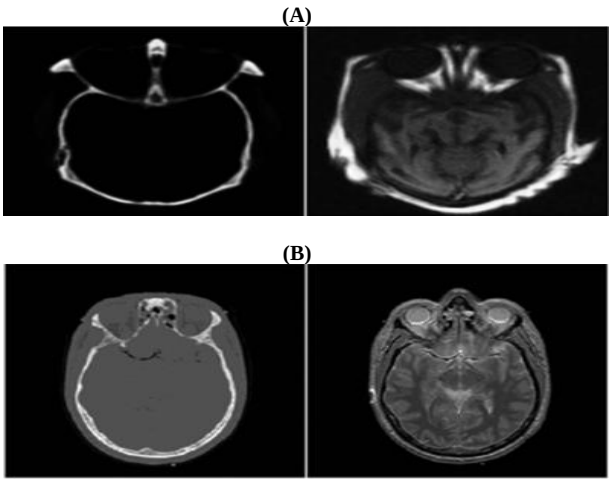


Fig. 1: CT and MR Images A) Dataset 1 B) Dataset 2.

In this work, we focused on fusion of CT and MR images of human brain and human abdomen. There has been tremendous boost in the research filed of medical image fusion and the publications also been increased. This enhancement in this context

Copyright © 2018 Suneetha Rikhari, Sandeep Jaiswal. This is an open access article distributed under the Creative Commons Attribution License, which permits unrestricted use, distribution, and reproduction in any medium, provided the original work is properly cited.

is mainly regulated by the medical diagnostic devices advanced usage, improved belief in the methodologies of medical diagnostics, fast growth of low-cost computing and imaging technologies.

In this, a Novel Implementation of Medical Image Registration and Fusion using ASM-SSIF is introduced, which will be formulated as a convex optimization problem by minimizing a linear combination of a least squares fitting term and an Active Slope Meagerness (ASM) regularizer with statistics based steered image filtration (SSIF). The work can be summarized as follows:

- A Novel utilization of ASM and SSIF for extracting the features from the input MR and CT images to be registered and fused. As per the author's best knowledge, this combo hasn't been utilized in image registration and fusion applications yet.
- A Fully new registration and fusion frame work is introduced based on proposed hybrid methodology. We mainly focused on the proper registration of medical images and then fusion of those registered images.
- We proposed simultaneous registration of two images during the fusion process, accomplished by ASM.
- We considered several quality indexes to disclose the effectiveness and robustness of proposed fusion model.

Rest of the paper structure is as follows: section 2 describes the related work done so far. Section 3 describes the proposed hybrid methodology ASM-SSIF. Section 4 includes results and discussion. Section 5 comprises the conclusions and the future enhancements.

2. Related work

Image registration in general and it's widely analyzed issue in medical imaging field. Author in [9] demonstrated similarity measurements and features based survey on the general image registration methods, which includes discourse on methodologies to detect the features and corresponding, implementation of a function coping with, transformation of an image and re-sampling. They also disclosed the performance evaluation of area and feature based registration methods. In [10], Wyawahare et al. presented innovative registration approaches. A substantial contribution of registration of images in medical literature concentrates on MR, CT imaging and other modalities of radiology. A panoptic survey made in [11], which considered the registration approaches of MR and CT imaging by dealing with different models such as mono and multi to model registration. Fixed or rigid feature-based approaches have been demonstrated in [12]. They also examined similarity-based approaches with intra model and intermodal (voxel). A registration approach based on group wise non-rigid has been presented by Bhatia et al. [13], which also provides a novel similarity metric with quantitative and qualitative analysis. All these are made for only MR and imaging. In [14] different sort of registration strategies has been presented by Markelj et al., such as gradient, intensity and feature, projection, back-projection and reconstruction-based strategies. Geometric transformations with optimized and similarity metrics in [15] described by Oliveira and Tavares. Further, they also verified all the software and methods of registration for evaluating the performance of proposed approaches. To deal with the variation of inter-person and altering the organs actively, the deformable transformation models utilized widely in the anatomy. These sorts of approaches have been presented in [16], which provides the summery of deformable registration. Registration models with Non-rigid transformation that includes splines and demons are also examined. The similar approach has been examined by Sotiras et al. in [17], which described the huge measure of deformable registration approaches, classified by the models of deformation, matching standard and utilized optimization techniques. While not restricted to the area of specific application, the examination puts vehemence on cope with the medical image registration approaches. Production of various number of spectral channels will be done by Spectral imaging, which gives the vital and very in detailed information when compared to the conventional gray scale image i.e., single channel image or a three-channel red-green-blue (RGB) image. The approaches for spectral image registration are given in [18–20]. However, most of the spectral image registrations approaches have been done on remote sensing imaging that are acquired from the long distance. While the major contribution of registration of medical images is concentrated on radiological modalities, methods for fusion of registered images have also been studied. In this perspective, several pixel-level image fusion techniques [8] were developed for the spatially registered images. Some are based on nonlinear operator, optimization based approaches, artificial neural network, multi resolution decomposition, and edge preserving-based methods. The nonlinear methods use min, max and morphological nonlinear operators for fusion which are discussed in [21] and [22]. Although these methods are simple and easy to employ they doesn't give good quality image output. Bayesian optimization problem is used in optimization-based approaches [23], which is in general, difficult to resolve. Hence, Markov random field [24] and generalized random walk [25] methods are used which computes edge aligned weights for solving the problem. These aligned weights are obtained after multiple iterations of the algorithm. But, because of multiple iterations over smoothed fused image may be obtained. Artificial neural networks based fusion techniques are also gaining much interest in the field of image fusion, which are discussed in [26-28]. In addition to the methods discussed, multi resolution schemes such as image pyramid and wavelet decomposition have also gained interest in the image fusion area. Image pyramid and wavelets requires the analysis in the frequency domain. Image pyramid splits the given input image into set of low-pass filtered images which are useful in representing the given input image at different scales [29-31]. Another category of multi resolution scheme utilizes discrete wavelet transform (DWT) [31-33]. DWT overcomes image pyramid by providing compact and directional information of a given image. DWT also gives less blocking effects than image pyramids. But, the shift invariant property of DWT may introduce artifacts. Hence to reduce artifacts obtained by DWT, stationary wavelet transform (SWT) has come into the research area of fusion [34]. Singular value decomposition (SVD) [35], high order singular value decomposition [36], and two-scale fusion (TIF) [37] are the recent techniques in the image fusion area. On more category of fusion techniques includes edge preserving methods such as L0-gradient minimization [38], weighted least filter [39], guided image filters (GFF) [40], and anisotropic diffusion [41]. For extracting salient information like lines and details edge preserving techniques are best suited in comparison to multiscale decomposition techniques. Because of linear filtering Pyramid decomposition may produce halo effects near the edges but with the use of nonlinear filtering, edge preserving techniques doesn't produce any halo effects.

3. Proposed frame work

As discussed earlier, constructing a well informative and representative image from number of images is known as fusion of images. Ideally, there are few steps that could help the users to obtain such goal by utilizing the fusion procedure. To implement those steps for the fusion of medical images, some considerations will be there. Precise registration is needed by the MR and CT image fusion, while the misalignment is quite hard to obviate during the preprocessing step. To surmount this, we had proposed a robust and new approach for both registration as well as the fusion of MR and CT images. This section briefly describes the major concepts involved in the proposed ASM-SSIF procedure. In this, image registration during the process of fusion is proposed. The registration is obtained by the ASM. Initially, the MR image is focalized to enhanced resolution, which permits us for more precise registration of images. At the same time, fusion

of images can be done precisely by extinguishing the misalignment gradually. We iteratively persist these two procedures until the convergence. Moreover, ASM method comprises the underlying correlation of various directions in images, which has been seldom before.

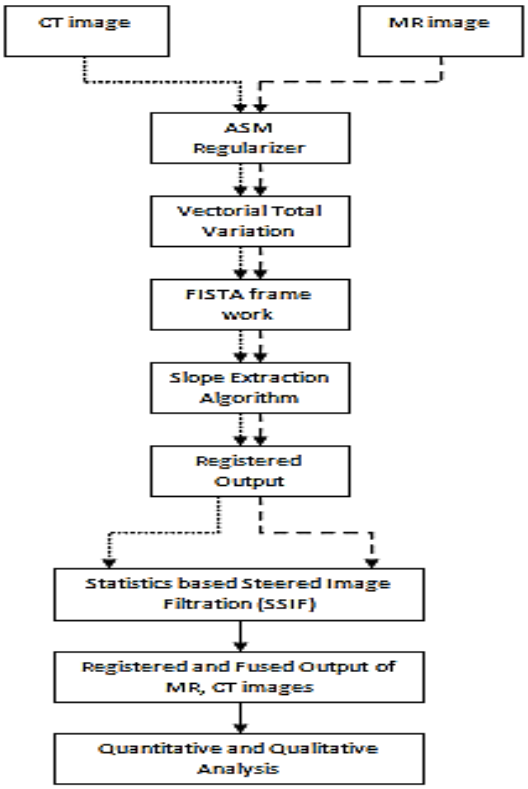


Fig. 2: Proposed Flowchart of Image Registration and Fusion Process Using ASM-SSIF.

Novel implementation called proximal slope algorithm has been developed for the overall energy function optimization. Particularly, we efficiently resolved the sub problems by employing the algorithm presented in [42], which was known as fast iterative shrinkage-thresholding algorithm (FISTA), and slope extraction method with backtracking, respectively. Most of the state-of-art methods extracted the spatial information from the MR images by utilizing the up-sampling approach. Anyways, the output obtained by this process is quite blurry and is not as much as enough accurate. Thus, we considered only down sampled MR image which is having close similarity to the original MR image. To give an example for this relationship, a least squares fitting concept is utilized:

$$\mathbb{E}_1 = \frac{1}{2}\|\Psi\mathbb{F} - \mathbb{M}\|^2 \quad (1)$$

Where, the operator for down sampling has been represented as Ψ, and the given eq. (1) significantly mitigates the distortion in the result. Understating E_1 could be a critically ill-posed issue, due to small down sampling rate. Without potent anterior information, estimation of accurate F is almost impossible.

3.1. Active slope meagerness

Precise registration is needed by the MR and CT image fusion, while the misalignment is quite hard to obviate during the preprocessing step. To assess the (dis) similarity, energy function is the most indispensable portions of image registration approaches. The proper coalition of images will be represented by a similarity optimization. In past, several similarity measurements have been widely utilized in the literature such as mutual information (MI), residual complexity (RC), correlation coefficient (CC), sum-of-squared-difference (SSD), and sum-of-absolute value (SAD). Almost all the conventional similarity measures are based on the values of pixels, when the images to be fused or registered have the standardized intensity fields. However, due to the different illumination conditions, the intensity fields of medical images may vary significantly. Most of the conventional similarity measurements based on the intensity is not strong enough to such distortions. Registering the input images is the first step in image fusion. Considering the medical images with large size, there is a requirement of similarity measurement stabilization without inaugurating higher complexity in computations. Hence, ASM is utilized to retain the information which is spatial in nature. Any misalignment will enhance the meagerness of the slopes. Therefore, the ASM can be naturally utilized as a similarity measurement. Now, the energy function is revised as:

$$E(F, T) = 1/2\ \|\Psi F - M\|^2 + \xi\|\nabla F - \nabla C^{-}(T)\| \quad (2)$$

Where ξ is a positive parameter, C^{-} means duplicating C, which is known as CT image. Interestingly, the obtained output will be similar to that of vectorial total variation (VTV) [43-44], when there is no reference image. This VTV is used for image de noising, de-blurring and reconstruction of images. The estimation of transformation is denoted as T. As the above function value is the addition of each pixel cost, this may lead to image overlapping. To obviate such a trivial solution, rather diminishing the value of energy function we utilized the slope extraction (SE) method. We detect that this can effectively obviate the iterative transforming of and image into the wrong direction. Now our objective is to mitigate the energy function (2). The solution to this problem is to fix T with respect to F and then do the vice-versa i.e. solve T by fixing F. For the F sub problem:

$$\mathbb{E}(\mathbb{F}) = \frac{1}{2}\|\Psi\mathbb{F} - \mathbb{M}\|^2 + \xi\|\nabla\mathbb{F} - \nabla\bar{\mathbb{C}}(T)\| \quad (3)$$

It is a provable function of convex. The first term is smooth while the second term is non-smooth, which actuates us to resolve this issue in FISTA [42] approach. For the first order methods, FISTA can obtain the optimal convergence rate. The T sub problem can be written as:

$$min\ \mathbb{E}(T) = \|\nabla\mathbb{F} - \nabla\bar{\mathbb{C}}(T)\| \quad (4)$$

Algorithm 1: ASM

Input: $\mathcal{L}, \xi, t^1 = 1, \mathbb{Y}^0$

for $i = 1$ to $Maxiteration$ do

$\mathbb{Y} = \mathbb{Y}^i - \Psi^{-1}(\Psi\mathbb{F} - \mathbb{M})/\mathcal{L}$

$\mathbb{F}^i = arg\ min_F \left\{\frac{\mathcal{L}}{2}\|\mathbb{F} - \mathbb{Y}\|^2 + \xi\|\nabla\mathbb{F} - \nabla\bar{\mathbb{C}}(T)\|\right\}$

$T = arg\ min_T\{\mathbb{E}(T) = \|\nabla\mathbb{F}^i - \nabla\bar{\mathbb{C}}(T)\|\}$

$t^{i+1} = \left[1 + \sqrt{1 + 4(t^i)^2}\right]/2$

$\mathbb{Y}^{i+1} = \mathbb{F}^i + \frac{t^i - 1}{t^{i+1}}(\mathbb{F}^i - \mathbb{F}^{i-1})$

end

Where Ψ^{-1} denotes inverse of Ψ. $\mathcal{L}$ is the Lipschitz constant for $\Psi^{-1}(\Psi\mathbb{F} - \mathbb{M})$. The result is updated based on both $\mathbb{F}^i$ and $\mathbb{F}^{i-1}$, while earlier methods updates $\mathbb{F}$ only based on $\mathbb{F}^i$. This is the main reason why the proposed method converges faster.

$$\mathbb{F}^i = arg\ min_F \left\{\frac{1}{2}\|\mathbb{F} - \mathbb{Y}\|^2 + \xi\|\nabla\mathbb{F} - \nabla\bar{\mathbb{C}}(T)\|\right\} \quad (5)$$

The VTV denoising algorithm is accelerated based on the FISTA framework to solve (5).The second sub problem (4) is solved with the SE method by backtracking. Let $\mathbb{r} = \nabla\mathbb{F} - \nabla\bar{\mathbb{C}}(\mathrm{T})$ be the residual and the tight approximation for the function:

$$\mathbb{E}(T) \approx \sum_m \sum_n \sqrt{\left(\nabla_1 \mathbb{r}_{m,n}\right)^2 + \left(\nabla_2 \mathbb{r}_{m,n}\right)^2 + \varsigma} \quad (6)$$

Where ς is a tiny constant ($\approx 10^{-10}$).
The transformation of an image is nonlinear. Here, we use the first order Taylor approximation that $\nabla\bar{\mathbb{C}}(\mathrm{T} + \Delta\mathrm{T}) \approx \nabla\bar{\mathbb{C}}(\mathrm{T}) + \mathfrak{J}\Delta\mathrm{T}$, where $\mathfrak{J}$ is the image Jacob of $\nabla\bar{\mathbb{C}}(\mathrm{T})$. Now, it is easy to obtain the slope of the energy function with respect to $\Delta\mathrm{T}$ by the chain rule. T can be updated iteratively with $\Delta\mathrm{T}$. Now warp the image with T to obtain a new Jacob matrix until convergence.

$$\Delta T = \mathfrak{J}^T \left(\frac{\partial \mathbb{E}(T)}{\partial \mathbb{r}}\right)$$

SE algorithm with backtracking is used to minimize the energy function (6), which is summarized in Algorithm 2. We set the initial step size $\mathfrak{t}^0 = 1$ and $\Omega = 0.8$. One can clearly observe that the linear operation is used in this approach by employing the Hierarchical estimation for the registration of medical images. The value of eq. (6) will be calculated on the both MR and CT images overlapping area. To obviate trivial solutions, here we utilized the normalized function values. This function value will be ∞ when there is no overlapping. We detected that this implementation could effectively obviate the trivial solutions.

Algorithm 2: SE with backtracking

Input: $\mathbb{F}$, $\mathcal{D}(\mathbb{C})$, $\mathfrak{t}^0$, $\Omega < 1$, T^0, $i = 0$

Repeat

Step 1: compute $T^{i+1} = T^i + \mathfrak{t}^i \Delta T^i$

Step 2: if $E(\mathrm{T}^{i+1})/\mathcal{O}_{i+1} > E(\mathrm{T}^i)/\mathcal{O}_i$, set $\mathfrak{t}^i = \Omega\mathfrak{t}^i$

and go back to step 1

Step 3: $\mathfrak{t}^{i+1} = \mathfrak{t}^i$

Step 4: $i = i + 1$

until Stop criterion is met

3.2. SSIF Procedure: the proposed SSIF method is explained as follows

If $\mathbb{S}$ is a steered image centered at a pixel $\mathcal{m}$ in a local square window $\mathcal{w}$, then the filtered output $\mathbb{O}$ at a pixel $\mathcal{n}$ is given by

$$\mathbb{O}_n = a_m \mathbb{S}_n + b_m, \forall n \in \mathcal{w}_m \quad (7)$$

Where a_m and b_m are the linear coefficients which are constant in window $\mathcal{w}_m$. Constraints are to be derived from input image $\mathbb{I}$ to determine the linear coefficients. The undesirable components $\mathbb{N}$ (like noise or texture) must be subtracted from $\mathbb{I}$ to obtain noise free filtered output,

$$\mathbb{O}_n = \mathbb{I}_n - \mathbb{N}_n \quad (8)$$

The difference between $\mathbb{I}$ and $\mathbb{O}$ can be minimized by maintaining the relation in eq. (7). Hence we can say that a_m and b_m are the linear coefficients that can reduce the cost function in window $\mathcal{w}_m$ as

$$E(a_m, b_m) = \sum_{n \in w_m} ((a_m \mathbb{S}_n + b_m - \mathbb{I}_n)^2 + \mathcal{r} {a_m}^2) \quad (9)$$

Where $\mathcal{r}$ is the regulization parameter. Eq. (9) represents the linear regression model. The solution for this is directly given by

$$a_m = \frac{\frac{1}{|w|}\sum_{n \in w_m} \mathbb{S}_n \mathbb{I}_n - \mu_m \bar{\mathbb{I}}_n}{{\sigma^2}_m + \mathcal{r}} \quad (10)$$

$$b_m = \bar{\mathbb{I}}_n - a_m \mu_m \quad (11)$$

Here $|\mathcal{w}|$ is the number of pixels in a window $\mathcal{w}_m$ centered at pixel $\mathcal{m}$, μ_m is the mean, and ${\sigma^2}_m$ is the variance in the window $\mathcal{w}_m$. $\bar{\mathbb{I}}_n$ is the mean of input $\mathbb{I}_n$ in $\mathcal{w}_m$ and is given by

$$\bar{\mathbb{I}}_n = \frac{1}{w}\sum_{n \in w_m} \mathbb{I}_n \quad (12)$$

After calculating linear coefficients, then output $\mathbb{O}_n$ can be solved according to eq. (7). Since overlapping windows $\mathcal{w}_m$ centered at $\mathcal{m}$ contain pixel $\mathcal{n}$ is common, average of all estimates of $\mathbb{O}_n$ is taken. Therefore the filtered output is

$$\mathbb{O}_n = \overline{a_m}\mathbb{S}_n + \overline{b_m} \quad (13)$$

Where $\overline{a_m} = \frac{1}{w}\sum_{n \in w_m} a_m$ and $\overline{b_m} = \frac{1}{w}\sum_{n \in w_m} b_m$ are the averages of the linear coefficients a_m and b_m respectively. In this article, filtering output of steered image $\mathbb{I}$ in the steering of $\mathbb{S}$ is denoted as $SSIF_{\mathfrak{y},\mathcal{r}}(\mathbb{I}, \mathbb{S})$, where $\mathfrak{y}$ is the filter size/neighborhood size and $\mathcal{r}$ is the degree of smoothing/regularization parameter. These two parameters $\mathfrak{y}$ and $\mathcal{r}$ controls the behavior of SSIF. If the variance ${\sigma^2}_m$ of a steered image is greater than the threshold $\mathcal{r}$ i.e., $({\sigma^2}_m \geq \mathcal{r})$, within a window $\mathcal{w}_m$, then the pixel located at the center of the window doesn't change. Now, the weights are calculated from the horizontal and vertical edge strengths of a pixel. Consider matrix $\mathbb{Q}$ with row as observation and column as variable and determine its covariance matrix by

$$cov(\mathbb{Q}) = E[(\mathbb{Q} - E[\mathbb{Q}])(\mathbb{Q} - E[\mathbb{Q}])^T] \quad (14)$$

Calculate unbiased horizontal estimate of a covariance matrix at a pixel location (m, n) as

$$\mathfrak{U}_{\mathcal{E}_\mathrm{H}}^{m,n}(\mathbb{Q}) = \frac{1}{p-1}\sum_{\mathcal{k}=1}^{p} (\mathbb{Q}_\mathcal{k} - \overline{\mathbb{Q}})(\mathbb{Q}_\mathcal{k} - \overline{\mathbb{Q}})^T \quad (15)$$

Where $\mathbb{Q}_\mathcal{k}$ is the $\mathcal{k}^{th}$ observation of the p -dimensional variable and $\overline{\mathbb{Q}}$ is the average of the observation. The diagonal of $\mathfrak{U}_{\mathcal{E}_\mathrm{H}}^{m,n}(\mathbb{Q})$is a variance vector. Compute Eigen values $\lambda_{\mathcal{E}_\mathrm{H}}^{\mathcal{k}}$ of $\mathfrak{U}_{\mathcal{E}_\mathrm{H}}^{m,n}(\mathbb{Q})$. As the size of matrix is $p \times p$, number of Eigen values can be found is p. By adding all the Eigen values the horizontal edge strength $\mathfrak{e}_{\mathcal{E}_\mathrm{H}}$ can be calculated.

$$\mathfrak{e}_{\mathcal{E}_\mathrm{H}}(m, n) = \sum_{\mathcal{k}=1}^{p} \lambda_{\mathcal{E}_\mathrm{H}}^{\mathcal{k}} \quad (16)$$

Similarly, for taking vertical edge strength into account calculate the unbiased vertical estimate $\mathfrak{U}_{\mathcal{E}_\mathcal{v}}^{m,n}$, and then compute the Eigen values $\lambda_{\mathcal{E}_\mathcal{v}}^{\mathcal{k}}$. All the Eigen values are added to get the vertical edge strength $\mathfrak{e}_{\mathcal{E}_\mathcal{v}}$as,

$$\mathfrak{e}_{\mathcal{E}_\mathcal{v}}(m, n) = \sum_{\mathcal{k}=1}^{p} \lambda_{\mathcal{E}_\mathcal{v}}^{\mathcal{k}} \quad (17)$$

The weight $\mathbb{W}(m,n)$of a pixel at location(m,n) is calculated by obtaining the sum of $\mathfrak{E}_{\mathcal{E}_H}(m,n)$ and $\mathfrak{E}_{\mathcal{E}_V}(m,n)$

$$\mathbb{W}(m,n) = \mathfrak{E}_{\mathcal{E}_H}(m,n) + \mathfrak{E}_{\mathcal{E}_V}(m,n) \quad (18)$$

To assign the weights adaptively, the process has to be repeated for each and every pixel in the image. Here, the weight of a pixel does not depend on its intensity value but its depends on its edge strength

4. Results and discussion

All the experiments have been done in MATLAB. The robustness of proposed algorithm with the real/natural images is shown in figure 3. In this section, we have represented both visual quality and quantitative analysis of various algorithms such as, Wavelet based methods decimated Wavelet Transform (D-WT) and Un-decimated wavelet transform (UWT), fast discrete Curvelet transform (FDCT) and multi-resolution singular value decomposition (M-SVD). Analysis of fusion metrics along with image quality assessment (IQA) metrics such as peak signal-to-noise ratio (PSNR), structural similarity index (SSIM), correlation coefficient (CC), root mean square error (RMSE) and entropy (E) are used to check the efficiency of the proposed ASM-SSIF algorithm. The metric with the best value is represented in bold case letter. Visual quality of fused images obtained using state-of-art algorithms such as PCA, DWT [33], UDWT, FDCT [46], M-SVD [35] and our method are demonstrated in figure 4 and figure 5 with data set 1 and data set 2 respectively. We can clearly observe that the perceptual quality of fused output using PCA, shown in figure 4(a) looks like low resolute image and the gray levels are not up to the mark. Other transformation methods like the methodology proposed in [33], UDWT and the algorithm demonstrated in [46] shown in figure 4(b-d) respectively, which performed superior to the PCA method in terms of visual perception, however these methods suffer from lack of contrast and edge preservation. Figure 4 (e) shown that the fused output of the method presented in [35], which was far better than the above-mentioned algorithms. However, all the existing fusion methods outputs not good at visual perception and lack of contrast with edge information. Our proposed method presented in figure 4(f), which looks more quality in visualization and good contrast with proper edge information. We also observe that this image has proper alignment of both CT and MR images of data set1; where as in figure 4(a-e) has not aligned properly.

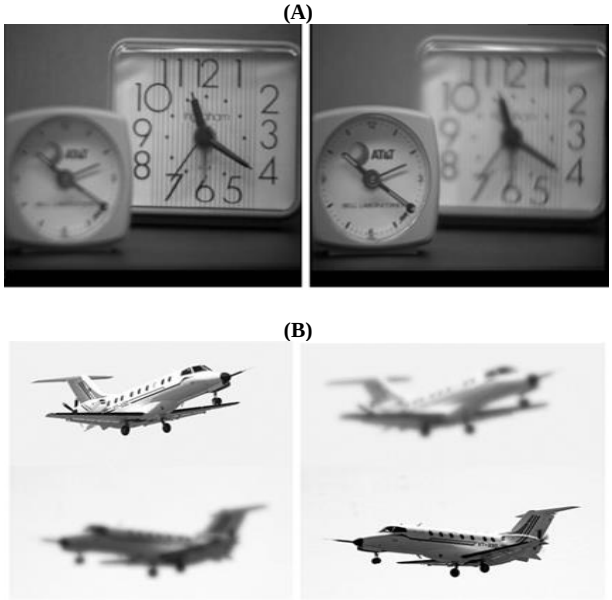


Fig. 3: A) Clock Data Set B) Airplane Data Set.

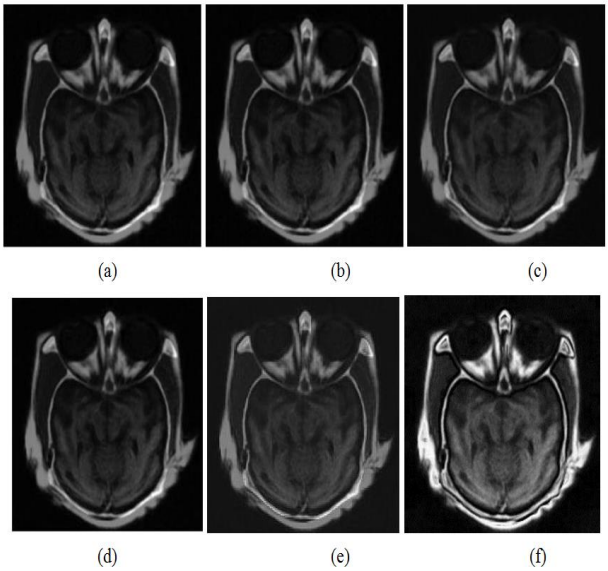


Fig. 4: Visualization of Fused Output Images with Data Set 1 A) PCA B) DWT C) UDWT D) FDCT (E) M-SVD and F) Proposed ASM-SSIF Method.

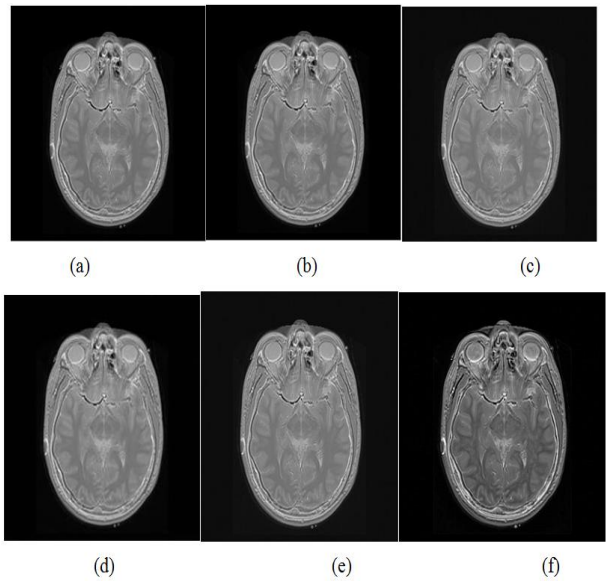


Fig. 5: Visualization of Fused Output Images with Data Set 2 (A) PCA B) DWT C) UDWT D) FDCT E) M-SVD and F) Proposed ASM-SSIF Method.

Table 1: Quantitative Analysis of Fusion Methods for Dataset 1

Methodology	PSNR (in dB)	RMSE	CC	SSIM	Entropy
PCA	67.595	0.106	0.888	0.9989	6.549
UDWT	62.253	0.1967	0.7928	0.986	6.11
DWT [33]	62.257	0.1966	0.7935	0.986	6.099
FDCT [46]	65.156	0.140	0.9206	0.9983	5.963
NSCT [45]	67.159	0.111	0.948	0.9987	6.62
M-SVD [35]	64.96	0.143	0.915	0.997	5.97
Proposed ASM-SSIF	91.31	0.0069	0.999	1	6.98

Table 2: Quantitative Analysis of Fusion Methods for Dataset 2

Meth-odol-ogy	PSNR (in dB)	RMSE	CC	SSIM	En-tropy
PCA	74.937	0.0456	0.978	0.999	4.637
UDWT	68.95	0.0909	0.933	0.988	0.9684
DWT [33]	68.98	0.0906	0.934	0.988	0.9683
FDCT [46]	70.215	0.140	0.9206	0.9983	5.05
NSCT [45]	75.159	0.0486	0.98	0.999	5.09
M-SVD [35]	74.932	0.0457	0.9785	0.999	4.9
Pro-posed ASM-SSIF	∞	0.00	1	1	5.22

Figure 5. (a-f) demonstrated that the PCA, DWT, UDWT, FDCT, M-SVD and our proposed method fused outputs with data set 2. The same analysis which we have discussed above has applicable for this also. The figure 5(f) show the clear view of both CT and MR images with good quality and proper alignment. The outputs of both registered and fused images of dataset 1 and dataset 2 obtained using proposed frame work has been presented in figure 6 and figure 7. Demonstration of registered and fused images using proposed algorithm has given in figure (c-d), where as in figure (a-b) shown that the input CT and MR images respectively.

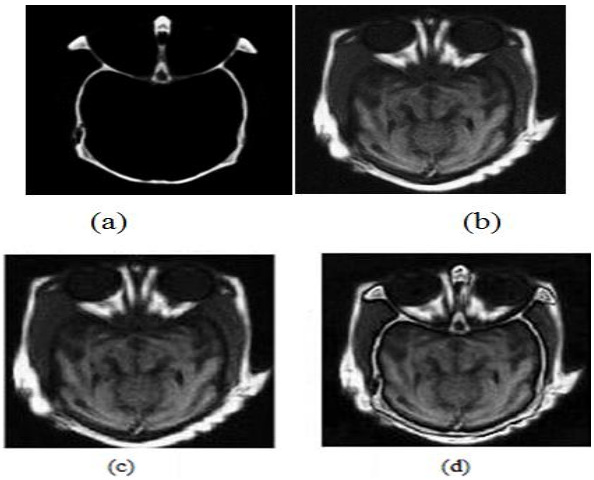


Fig. 6: A) CT Image B) MR Image C) Registered Image and D) Fused Image Using Proposed ASM-SSIF Method.

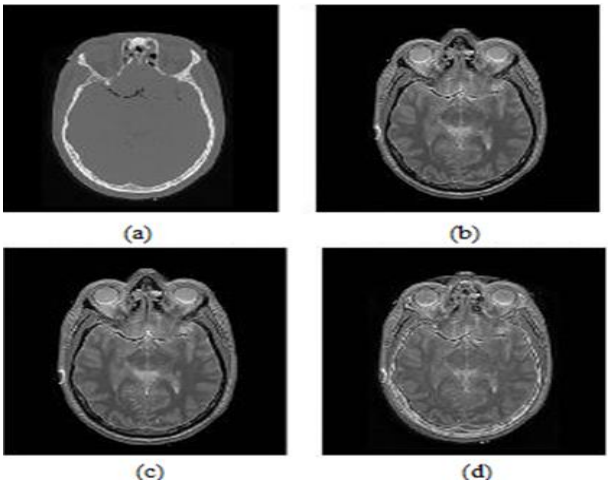


Fig. 7: A) Ct Image B) MR Image C) Registered Image and D) Fused Image Using Proposed Asm-Ssif Method.

Quantitative analysis with IQA shown in table 1 for the test results presented in figure 4, which gives the analysis of dataset 1. Table 1 consists of various fusion metric parameters such as PSNR, RMSE, CC, SSIM and entropy. The best values are highlighted in bold letters. Our proposed method obtained far better values over all the existing fusion methods discussed in the literature. We also tested the qualitative analysis of dataset 2 with the similar fusion metric parameters considered for dataset 1.

5. Conclusions

In this, we proposed a novel implementation of medical image registration and fusion using Active Slope Meagreness (ASM) regularizer with statistics based steered image filtration (SSIF). Precise registration is needed by the MR and CT image fusion, while the misalignment is quite hard to obviate during the preprocessing step. To surmount this, we had proposed a robust and new approach for both registration as well as the fusion of MR and CT images. Our approach focuses on simultaneous registration during the fusion procedure. Initially, the MR image is focalized to enhanced resolution, which permits us for more precise registration of images. At the same time, fusion of images can be done precisely by extinguishing the misalignment gradually. We have run these two procedures iteratively until the convergence. Fusion performance is assessed using visual perception analysis and IQA with fusion metric parameters. Results showed that our algorithm is giving better performance by enhancing the overall fusion quality of MR and CT images in terms of IQA with fusion metric parameters. Specifically, our proposed ASM-SSIF method is shown to be much more powerful on medical data sets of real-world with pre-registration errors.

References

[1] Rajiv Singh, "Medical image fusion: applications, approaches and evaluation, in International conference on Medical Imaging and Diagnosis, Chicago, USA, (2016).

[2] Friston, K., Ashburner, J., Frith, C., Poline, J. Heather, J., & Frackowiak, R., "Statistical parametric maps in functional imaging: a general linear approach", Hum Brain Mapp 2, (2004), 189–210.

[3] Pengqiang, Z., Xuchu, Y., Li, H., & Lihua, S., "Automatic registration of airborne image sequences based on line matching approach", ISPRS 37, (2008).

[4] Sarvaiya, J., Patnaik, S., & Kothari, K., "Feature based image registration using Hough Transform", Surat, Gujarat, India: National Institute of Technology, (2013).

[5] Wang, X., Feng, D., & Jin, J., "Elastic Medical Image Registration Based on Image Intensity", Pan-Sydney Area Workshop on Visual Information Processing, Sydney: Australian Computer Society, (2001).

[6] Zheng, L.-T., Qian, G.-P., & Lin, L.-F., "Medical Image Registration Based on Improved PSO Algorithm", In J. Lee (Ed.), Advanced Electrical and Electronics Engineering, Lecture Notes on Electrical Engineering, Springer: Berlin Heidelberg, Vol. 87, (2011), 487–494.

[7] J. B. Antoine Maintz and Max A. Viergever, "A survey of medical image registration", Medical Image Analysis, Vol. 2, No. 1, (1998), 1-36.

[8] Hamza A, He Y, Krim H, Willsky A., "A multiscale approach to pixel-level image fusion", Integrated Computer. Aided Engineering, Vol. 12, No. 2, (2005), 135– 146.

[9] B. Zitova, J. Flusser, "Image registration methods: a survey", Image and Vision Computing, Vol. 21, No. 11, (2003), 977–1000.

[10] M. Wyawahare, P. Patil, H. Abhyankar, "Image registration techniques: an overview", International Journal of Signal Processing, Image Processing and Pattern Recognition, Vol. 2, No. 3, (2009), 11–28.

[11] J.B. Antoine Maintz , Stefan Klein , Keelin Murphy , Marius Staring , Josien P.W. Pluim, "A survey of medical image registration – under review", Medical Image Analysis, Vol. 33, (2016), 140-144.

[12] D. Hill, P. Batchelor, M. Holden, D. Hawkes, "Medical image registration", Physics in Medicine and Biology, Vol. 46, No. 3, (2001), 1-45.

[13] K. Bhatia, J. Hajnal, A. Hammers, D. Rueckert, "Similarity metrics for group wise non-rigid registration", In: Proceedings of Medical

Image Computing and Computer-Assisted Intervention (MICCAI), Springer, (2007), 544–552.
[14] P. Markelj, D. Toma ˇ Zevi ˇ c, B. Likar, F. Pernu ˇ s, "A review of 3D/2D registration methods for image-guided interventions", Medical Image Analysis, Vol. 16, No. 3, (2012), 642–661.
[15] F.P. Oliveira, J.M.R. Tavares, "Medical image registration: a review", Computer Methods in Biomechanical and Biomedical Engineering, Vol. 17, No. 2, (2012), 73–93.
[16] W. Crum, T. Hartkens, D. Hill, "Non-rigid image registration: theory and practice", Br. J. Radiol. Vol. 77, (2004), 140-153
[17] A.Sotiras, C. Davatzikos, N. Paragios, "Deformable medical image registration: a survey", IEEE Transactions on Medical Imaging, Vol. 32, No. 7, (2013), 1153–1190.
[18] H. Stone, R. Wolpov, "Blind cross-spectral image registration using pre-filtering and Fourier-based translation detection", IEEE Transactions Geoscience and Remote Sensing, Vol. 40, No. 3, (2002), 637–650.
[19] M. Pfingsthorn, A. Birk, S. Schwertfeger, H. Bülow, K. Pathak, "Maximum likelihood mapping with spectral image registration", Proceedings of IEEE International Conference on Robotics and Automation (ICRA), Anchorage, USA, (2010), 4282–4287
[20] M. Hasan, X. Jia, A. Robles-Kelly, J. Zhou, M.R. Pickering, "Multi-spectral remote sensing image registration via spatial relationship analysis on sift key points", Proceedings of IEEE International Geoscience and Remote Sensing Symposium (IGARSS), Honolulu, USA, (2010), 1011–1014.
[21] De I, Chanda B, Chattopadhyay B, "Enhancing effective depth-of-field by image fusion using mathematical morphology", Image and Vision Computing, Vol. 24, No. 12, (2006), 1278–1287.
[22] Yang B, Li S, "Multi-focus image fusion based on spatial frequency and morphological operators", Chinese Optical Letters, Vol. 5, No. 8, (2007), 452–453.
[23] Fasbender D, Radoux J, Bogaert P., "Bayesian data fusion for adaptable image pan sharpening", IEEE Transactions on Geoscience and Remote Sensing, Vol. 46, No. 6, (2008), 1847–1857.
[24] Shen R, Cheng I, Shi J, Basu A. Generalized random walks for fusion of multi-exposure images. IEEE Transactions on Image Processing, Vol.20, (2011), 3634–3646.
[25] Xu M, Chen H, Varshney PK, "An image fusion approach based on Markov random fields", IEEE Transactions on Geoscience and Remote Sensing, Vol. 49, No. 12, (2011), 5116–5127
[26] Hong Zhang, Xiao-Nan Sun, Lei Zhao, Lei Liu, "Image Fusion Algorithm Using RBF Neural Networks", In 3rd International Workshop on Hybrid Artificial Intelligence Systems, Lecture Notes in Computer Science, (2008), 417-424.
[27] Hong Jiang, Yufen Tian, "Fuzzy image fusion based on modified Self-Generating Neural Network", Expert Systems with Applications, Vol. 38, No. 7, (2011), 8515-8523.
[28] Nianyi Wang, Yide Ma, Kun Zhan, "spiking cortical model for multi focus image fusion", Neurocomputing, Vol. 130, (2014), 130: 44-51.
[29] Peter J. Burt, Edward H. Adelson, "The Laplacian Pyramid as a Compact Image Code", IEEE Transactions on Communications, Vol. 31, No. 4, (1983), 532-540.
[30] Akanksha Sahu, Vikrant Bhateja, Abhinav Krishn and Himanshi, "Medical Image Fusion with Laplacian Pyramids", In International Conference on Medical Imaging, m-Health and Emerging Communication Systems (MedCom), Greater Noida, India, (2014), 448-453
[31] Hannandeep Kaur and Jyothi Rani, "Image Fusion on Digital images using Laplacian Pyramid with DWT", In 3rd International Conference on Image Information Processing, Waknaghat, India, (2015), 393-398.
[32] Deepali Sale, Varsha Patil, Dr. Madhuri A. Joshi, "Effective Image Enhancement Using Hybrid Multi Resolution Image Fusion", In IEEE Global Conference on Wireless Computing and Networking, Lonavala, India, (2014).
[33] Bhavana V and Krishnappa H K., "Multi-modality Medical Image Fusion Using Discrete Wavelet Transform", In 4th International Conference on Eco-friendly Computing and Communication Systems (ICECCS), Vol. 70, (2015), 625-631.
[34] M D Nandesh and M Meenakshi, "A Novel Technique of Medical Image Fusion Using Stationary Wavelet Transform and Principle Component Analysis", In International Conference on Smart Sensors and Systems (IC-SSS), Bangalore, Inida, (2015).
[35] V P S Naidu, "Image Fusion Technique Using Multi-resolution Singular Value Decomposition", Defense Science Journal, Vol. 61, No. 5, (2011), 479-484.
[36] Junli Liang, Yang He and Ding Liu., "Image Fusion Using Higher-order Singular Value Decomposition", IEEE Transactions on Image Processing, Vol. 21, No. 5, (2012), 2898-2909.
[37] Bavirisetti DP and Dhuli R., "Two-scale image fusion of visible and infrared images using saliency detection", Infrared Physics and Technology, Vol 76, (2016), 52–64.
[38] Zhao J, Feng H, Xu Z, Li Q and Liu T., "Detail enhanced multisource fusion using visual weight map extraction based on multi scale edge preserving decomposition", Optics Communications, Vol. 287, (2013), 45–52.
[39] Jiang Y and Wang M., "Image fusion using multiscale edge preserving decomposition based on weighted least squares filter", IET Image Processing, Vol. 8, No. 3, (2014), 183–190.
[40] Li S, Kang X, Hu J., "Image fusion with guided filtering", IEEE Transactions on Image Processing, Vol. 22, No. 7, (2013), 2864–2875.
[41] Bavirisetti DP and Dhuli R. "Fusion of infrared and visible sensor images based on anisotropic diffusion and Karhunen-Loeve transform", IEEE Sensors Journal, Vol. 16, No. 1, (2016), 203–209.
[42] A.Beck and M. Teboulle, "A fast iterative shrinkage-thresholding algorithm for linear inverse problems", SIAM Journal on Imaging Sciences, Vol. 2, No. 1, (2009), 183–202.
[43] J. Huang, C. Chen, and L. Axel, "Fast Multi-contrast MRI Reconstruction", Magnetic Resonance Imaging, Vol. 32, No. 10, (2012), 1344-1352.
[44] C. Chen, Y. Li, and J. Huang, "Calibration less Parallel MRI with Joint Total Variation Regularization", In International Conference on Medical Image Computing and Computer-Assisted Intervention, Lecture Notes in Computer Science, Springer, Vol. 8151, (2013), 106–114
[45] L Zhan and XiuXia Ji, "CT and MR Images Fusion Method based on Non-sub sampled Contourlet Transform", In 8th International Conference on Intelligent Human-Machine Systems and Cybernetics, Hangzhou, China, (2016), 257-260.
[46] C V Rao, J Malleswara Rao, A Senthil Kumar, D S Jain and V K Dhawal, "Satellite image Fusion using Fast Discrete Curvelet Transforms", In IEEE International Advance Computing Conference, Gurgaon, India, (2014). 952-957.